Nature Environment and Pollution Technology
An International Quarterly Scientific Journal
p-ISSN: 0972-6268
(Print copies up to 2016)
e-ISSN: 2395-3454
Vol. 25 | No. 3 | Article ID B4394 | 2026
Original Research Paper
https://doi.org/10.46488/NEPT.2026.v25i03.B4394
Open Access Journal

Central Composite Design-Based Optimization of Heterogeneous Fenton-Like Catalytic Oxidation of Real Pharmaceutical Wastewater Using Cu-Fe/SiO_2

Neha Kulshreshtha, Vishal Kumar Sandhwar†, Alok Tiwari and Shivendu Saxena
Department of Chemical Engineering, Parul Institute of Technology, Parul University, Vadodara-391760, Gujarat, India
†Corresponding author: Vishal Kumar Sandhwar; vishal.sandhwar8850@paruluniversity.ac.in

Abbreviation: Nat. Env. & Poll. Technol.
Website: www.neptjournal.com

Received: 08-09-2025
Revised: 12-12-2025
Accepted: 14-12-2025

Key Words:

Pharmaceutical wastewater
COD removal
Catalytic oxidation
Cu-Fe/SiO_2
Process optimization

Citation for the Paper:

Kulshreshtha, N., Sandhwar, V.K., Tiwari, A. and Saxena, S., 2026. Central composite design-based optimization of heterogeneous Fen-ton-like catalytic oxidation of real pharmaceutical wastewater using Cu-Fe/SiO_2. *Nature Environment and Pollution Technology*, 25(3), B4394. https://doi.org/10.46488/NEPT.2026.v25i03.B4394

Note: From 2025, the journal has adopted the use of Article IDs in citations instead of traditional consecutive page numbers. Each article is now given individual page ranges starting from page 1.

ABSTRACT

This research explores heterogeneous Fenton-like catalytic oxidation for the treatment of actual pharmaceutical wastewater with Cu–Fe supported on SiO_2 as an active catalyst. Catalyst preparation and characterization via X-ray diffraction (XRD), scanning electron microscopy (SEM), Fourier-transform infrared (FTIR) spectroscopy, and BET analysis for porosity, crystallinity, and active site distribution were completed. To optimize treatment parameters, response surface methodology using central composite design (CCD) investigated catalyst dosage, H_2O_2 concentration, initial pH, and reaction time for the maximum chemical oxygen demand (COD) removal. The CCD determinant generated a quadratic model (R^2 = 0.9881) to predict experimental results, which, when confirmed via successful achievement of proposed conditions, resulted in 76.07% COD removal. This work indicates the efficiency, reproducibility and feasibility of scaling the Cu–Fe/SiO_2 catalyst for pharmaceutical wastewater treatment and is a step toward sustainability.

1. INTRODUCTION

The global rise of pharmaceutical production and consumption has led to billions of gallons of pharmaceutical wastewater (PWW) each year from industrial effluent release, making PWW one of the most complex industrial by-product issues to plague the discipline of environmental engineering and wastewater treatment. PWW is characterized by an extraordinarily high chemical oxygen demand (COD), often greater than 5,000 $mg.L^{-1}$ and a notorious brew of xenobiotics, recalcitrant and toxic organic pollutants. Specifically, PWW contains active pharmaceutical ingredients (APIs), antibiotics, solvents, EDCs, and sustainable agents such as surfactants and complexing agents. All of these are released into the environment at concentrations that cause acute and chronic toxicity to aquatic organisms, reduce microbial consortium operability, contribute to the presence of antibiotic-resistant genes (ARGs), and endanger public health and ecosystem stability. Unlike general municipal wastewater or the wastewater generated from other industries, PWW is defined by an unregulated profile and low biodegradability, similar to how drugs meant for human use are processed by the human body and excreted in a non-degraded state. Thus, this convoluted composite presents a severe problem for simple discharge into receiving waters that must now deal with such effluents and poses issues for agricultural systems that might apply non-treated water for irrigation and treatment and the resultant particles that become prolific transformation products (Fu et al. 2019, Luo et al. 2019, Ahidjo et al. 2024). Biological treatment options, such as activated sludge and anaerobic digestion, constitute the traditional means to extract organic pollutants from municipal and some industrial waste streams in ideal environments. Yet, this is not always the case, and without fail, biological treatment options require an emphasis on biodegradability. Therefore, such treatment options for pharmaceutical wastewater (PWW) are largely ineffectual. This occurs for two reasons: 1) toxic constituents within pharmaceutical wastewater inhibit biological activity, and 2) recalcitrant molecules preclude proper chemical oxygen demand (COD) removal, leading to more toxic, recalcitrant intermediates. Enhanced systems ranging from membrane bioreactors (MBRs) or hybrid solutions integrating biological stimulus and physicochemical phenomena yield superior effluent quality and favorable outcomes. Yet again, membrane bioreactors experience membrane fouling due to excess retained solids, or treatment enhancements fail in the face of antibiotics, pharmaceuticals and endocrine disrupting compounds (EDCs) constituting the real-life PWW (Nebot et al. 2015). The largest unresolved component is the failure to remove pharmaceuticals from the NGO flow post-treatment, as evidenced by WWTP analysis that determined many pharmaceutical compounds existed in both influent and effluent, despite average populations and more rural settings judging such results implausible within their community confines. Unfortunately, WWTPs have become considered an active avenue of pharmaceuticals entering the greater aqueous environment. Using sensitive detection variables, the same pharmaceutical remnants that entered the WWTP stream ended up in the effluent discharge. Therefore, new treatment methods for PWW need to be more efficient, reliable and cost-efficient (Dai et al. 2023, Alfarsi et al. 2025). Thus, Advanced Oxidation Processes (AOPs)—homogenous Fenton and Fenton-like processes present a feasible option for treatment alternatives under generating conditions. AOPs create a wealth of reactive hydroxyl radicals (-OH), which irreversibly degrade complex organic components into much smaller byproducts like H_2O and CO_2. However, the homogeneous Fenton reaction and its derivatives are limited beyond practical application to large-scale high-strength pharmaceutical waste streams. Fenton's reaction occurs at a strictly acidic pH (~pH 3) with an abundance of iron salts producing non-manageable sludges and a rapid deactivation/catalyst leaching phenomenon. These operational limitations increase overall treatment costs while generating residual management issues that negatively impact overall efficiency when neutral pH or cost efficacy is required for high-temperature industrial operations (Xu et al. 2022). To address these issues, the recent emergence of heterogeneously operating Fenton-like catalysts, largely due to bimetallic systems supported on high-surface-area substrates such as silica (SiO_2), has expanded the research and development behind advanced PWW treatment. One of the most promising such new materials includes Cu–Fe/SiO_2 catalysts, which utilize the bimetallic, synergistic redox cycling potential between copper and iron (i.e., Cu^{2+}/Cu^{+} and Fe^{3+}/Fe^{2+} transformations) to generate hydroxyl radicals over a milder range of conditions, including near-neutral pH. Furthermore, SiO_2 as a catalytic support aids in site dispersion, thermal and chemical stabilization of the catalytic structure, and porosity control, all necessary factors to promote effective contact with intended non-target species and efficient contaminant breakdown. In proof-of-concept studies, researchers note that the Cu–Fe/SiO_2 catalysts achieve rapid reaction rates and extents of organic and pharmaceutical contaminant removal, outperforming degradation efficiencies of traditional homogeneous endpoints and single-metal heterogeneous options. Central Composite Design (CCD) under Response Surface Methodology (RSM) provides a powerful solution to many of the optimization needs generated by complex systems. CCD allows for the exploration and modeling of independent operating variables and their interactions and attempts to find the optimal response conditions for pollutant removal (Sandhwar & Prasad 2017, Sandhwar & Prasad 2018, Luo et al. 2019, Kumar et al. 2021, Thomas et al. 2021, Xu et al. 2022, Dai et al. 2023, Yang & Xue 2024).

Quantitative performance comparison highlights limitations of existing benchmarks relative to real pharmaceutical wastewater treatment challenges. Fe/Cu composites achieved only 36% COD removal in real antibiotic wastewater under unspecified H_2O_2 and catalyst dosing conditions, demonstrating limited efficacy for complex pharmaceutical matrices. Homogeneous Fe^{2+}/H_2O_2 systems report 78.4% COD removal in real pharmaceutical wastewater using 1 mg, L^{-1} Fe^{2+} but generate problematic iron sludge and lack catalyst recyclability (Omar et al. 2024, Wang et al. 2025). FeCr-SBA-15/AC on SBA-15/activated carbon support delivers an impressive 97% removal, but targets synthetic methyl orange dye (single compound, easily degradable chromophore) rather than multi-component pharmaceutical effluents, with 0.75 $g.L^{-1}$ dosing and no H_2O_2 consumption reported. CuFe/SBA-15 catalysts show promise for model pollutants but provide no quantified COD removal data, H_2O_2 doses, or operational conditions, limiting benchmarking utility (Hamieh et al. 2025). CuO/Fe_3O_4/SiO_2 composites report qualitatively "high removal" for dyes without specific COD percentages, H_2O_2 consumption metrics, or catalyst loadings, precluding rigorous performance evaluation (Ngoc & Vu 2022). While many studies have reported on Cu-Fe catalysts, the present work is novel in terms of its actual application, support, and parameter optimization. First, many studies use prepared solutions of single pharmaceuticals, while this study tests an effective solution using real pharmaceutical wastewater, which includes many recalcitrant organic compounds and poses a much more difficult solution for Fenton-like oxidation (Chen et al. 2013, Nguyen et al. 2020, Thomas et al. 2021, Nam et al. 2025, Wang et al. 2025). Second, the catalyst is supported on SiO_2, which is a much less commonly used support than Al_2O_3, activated carbon, or magnetic ferrites. SiO_2 has increased surface dispersion characteristics and a structurally neutral disposition, which offer effective dispersive and Cu-Fe redox properties. Third, the parameters were optimized using central composite design (CCD) for real wastewater purposes and not synthetic pollutants to create greater observed relevance and applicability to actual industrial demand.

The present work envisages the synthesis of a Cu–Fe/sio₂ composite catalyst using the wet impregnation method and examines its efficiency for the treatment of real pharmaceutical wastewater via catalytic activation of hydrogen peroxide. The developed catalyst was characterized using different characterization techniques such as XRD, SEM, FTIR, and BET to understand its properties. To evaluate the effect of key operational parameters on COD removal efficiency, batch experiments were carried out based on the CCD framework. The developed statistical models inform the prediction and adjustment of reaction conditions for best performance. Ultimately, this study aims to facilitate an efficient catalytic reaction for the treatment of pharmaceutical wastewater with sustainability in mind to foster an effective new course of action for subsequent projects to improve environmental sustainability measures and safeguard public health. These findings show the advantages of a heterogeneous Fenton-like approach to safety and environmental quality with a more efficient, cost-effective, and sustainable approach to treating pharmaceutical wastewater.

2. MATERIALS AND METHODS

2.1. Chemicals

All chemicals, such as Copper (II) Nitrate Trihydrate ($Cu(NO_3)_2{\cdot}3H_2O$, Iron(III) Nitrate Nonahydrate ($Fe(NO_3)_3{\cdot}9H_2O$), Tetraethyl Orthosilicate (TEOS, $Si(OC_2H_5)_4$), Ethanol (C_2H_5OH), etc., used in this study were of analytical grade and used without further purification. The following chemicals were procured from Neelkanth Hari Chemical, Vadodara, Gujarat, India. All glassware and instruments used in the synthesis and analysis were thoroughly cleaned with chromic acid and rinsed with deionized water to prevent any contamination.

2.2. Characteristics of Pharmaceutical Industry Wastewater

The wastewater, which was treated in the catalytic oxidation processes, was supplied from a pharmaceutical plant located in Vadodara. The initial total dissolved solids, chemical oxygen demand, pH, biological oxygen demand, and turbidity of the wastewater were assessed and are detailed in Table 1. The samples were stored in a refrigerator at 4°C until use.

Table 1: Characterization of real pharmaceutical wastewater.

Sr. No.	Parameters	Unit [SI])	Measured Value
1.	pH		8.2
2.	Turbidity	NTU	28.40
3.	COD	$mg.L^{-1}$	6112
4.	BOD (3 days at 27 degrees Celsius)	$mg.L^{-1}$	2987
5.	Total dissolved Solid	$Mg.L^{-1}$	2780

2.3. Catalyst Preparation

The Cu–Fe/SiO_2 heterogeneous catalyst was synthesized via the wet impregnation method (Kumar et al. 2021), utilizing commercially available SiO_2 powder as a support. This method allows for facile preparation and effective dispersion of active metal species onto the support. Copper(II) nitrate trihydrate ($Cu(NO_3)_2{\cdot}3H_2O$) and iron (III) nitrate nonahydrate ($Fe(NO_3)_3{\cdot}9H_2O$) were obtained at stoichiometric amounts.

After accurate weighing, the weighed portions were dissolved in a minimal amount of deionized water to afford a mixed metal nitrate solution in aqueous form. The loading ratio of Cu: Fe was maintained at 1:1, and the total metal loading was calculated at 10 wt% of the total mass of the catalyst. To the metal nitrate solution obtained, commercial amorphous SiO_2 powder was added gradually with continuous stirring conducted at room temperature to ensure proper impregnation. After 4 h of stirring, the slurry was transferred to a Petri dish and dried in a hot air oven set at 110°C for 12 h. Upon drying, the resultant solid precursor was calcined in a muffle furnace at 500°C for 4 h in air to decompose the nitrates and yield the metal oxides (CuO and Fe_2O_3 or Fe_3O_4) with enhanced stability and strong adhesion to the surface of SiO_2. The resulting calcined catalyst was cooled to room temperature, ground into a fine powder, and stored in airtight containers for further experimentation in catalytic studies. The resultant catalyst is an active and stable Cu–Fe/SiO_2 for heterogeneous Fenton-like reactions of pharmaceutical wastewater treatment (Liu et al. 2024, Li et al. 2025).

The selected 1:1 Cu:Fe molar ratio was not arbitrary; it is widely reported to enhance Fenton-like activity due to the synergistic redox cycling between Cu^{2+}/Cu^{+} and Fe^{3+}/Fe^{2+}, which accelerates the generation of hydroxyl radicals (Chen et al. 2024, Wang et al. 2024, Hu et al. 2025). Several studies have shown that equimolar Cu–Fe compositions yield higher catalytic activity and stability compared to non-equimolar ratios because both metals participate simultaneously in electron transfer cycles (Vainoris et al. 2022, Kongkoed et al. 2024, Wang et al. 2024, Nam et al. 2025). Similarly, the 10 wt% total metal loading was selected based on literature indicating that loadings in the range of 8–12 wt% provide optimal dispersion of mixed metal oxides on oxide supports without causing pore blockage, crystallite overgrowth, or agglomeration (Munnik et al. 2015, Peralta-Ladino et al. 2025, Tajoli et al. 2025). Higher loadings (>15 wt%) often lead to particle sintering during calcination, while lower loadings (<5 wt%) can result in insufficient active sites (Bellouard et al., 2024; Khan et al., 2025). The molar concentration of the precursor solution was maintained at 0.5 M for both Cu and Fe salts to enable homogeneous impregnation while preventing oversaturation of the support surface. The impregnation step was conducted at the native solution pH, governed by the nitrate precursors; this pH range is appropriate for maintaining metal ions in soluble form and ensuring uniform distribution over SiO_2 without premature precipitation (Tricoli et al. 2010, Bravo-Suarez et al. 2025).

2.4. Catalyst Characterization

The structural, morphological and surface properties of Cu–Fe/SiO_2 were extensively examined and characterized via various instruments in order to understand the nature of the catalyst for in situ reaction. X-Ray Diffraction (XRD) was employed for crystallite structure and phase determination, where a D6 PHASER X-Ray Diffractometer (Bruker India Scientific Pvt. Ltd.) with Cu Kα radiation (λ = 1.5406 Å) in the 2θ range of 10°–80° was utilized for analysis. Fig. 1 represents the XRD spectrum of the synthesized catalyst. The XRD pattern for the synthesized Cu–Fe/SiO_2 catalyst indicates the presence of both amorphous and crystalline phases. The broad halo between 20–25° (2θ) is attributed to the formation of amorphous SiO_2, which corroborates the selection of silica as the support material for the catalyst. Superimposed crystalline features on the SiO_2 halo relate to the characteristic crystalline phases presumed from the presence of copper and iron oxides. The peaks corresponding to CuO (tenorite, monoclinic) are noted at 35.5°, 38.7°, and 48.7°, while the peaks appearing at about 30.2°, 35.6°, 43.3°, 57.3°, and 62.9° are attributed to Fe_2O_3 (hematite). Additionally, the overlapping peaks at 30.3°, 33.1°, and 51.4° indicate the presence of a $CuFe_2O_4$ spinel phase formed, which is a mixed Cu–Fe oxide phase that is commonplace in bimetallic systems. Thus, the presence of crystalline phases over the amorphous SiO_2 support indicates that the Cu and Fe species have been loaded successfully onto silica to provide many redox-active sites and maintain structural stability for effective heterogeneous Fenton-like catalysis (Ning et al. 2018, Ren et al. 2020, Pratiwi et al. 2021). Scanning Electron Microscopy (SEM) on an SU3800 Hi-SEM system (Hitachi High-Tech India Pvt. Ltd.) discerned particle morphology and distribution. Fig. 2 indicates an SEM micrograph. According to the SEM provided, the surface morphology of the catalyst is non-uniform as it appears to be comprised of irregularly shaped/agglomerated particles. They appear to be somewhat loosely packed, forming clusters/areas of rough and porous characteristics—ideal for enhancing surface area and possessing necessary active sites. The microstructure of Cu–Fe/SiO_2 is heterogeneous, as there are small, fragmented-like structures and large plate-like formations, which suggests that the metal oxides are dispersed nicely on the silica support. These structures are in line with what would be beneficial for mass transfer and catalytic activity because the roughness/pore openings allow easy access and engagement of the species with the catalyst surface. Thus, the SEM suggests that the catalysts are appropriately structured for heterogeneous Fenton-like catalytic activity for wastewater treatment (Martínez et al. 2017, Ning et al. 2018, Thomas et al. 2021). Fourier Transform Infrared Spectroscopy (FTIR) from a Bruker Alpha II FTIR spectrometer compiled via the KBr pellet technique in the wavenumber range of 400–4000 cm^{-1} determined surface functionality. Fig. 3 shows the FTIR spectrum. The FTIR spectrum of the Cu–Fe/SiO_2 catalyst (Fig.3) shows specific absorption bands, which indicate the formation of the silica support and metal oxides. The presence of silica is confirmed by a strong and broad band at 1080–1100 cm^{-1} with shoulders at 800 cm^{-1}, which relates to the asymmetric and symmetric stretching vibrations of Si–O–Si linkages. In addition, a weak band appears at 950–970 cm^{-1}, relating to Si–OH stretching vibrations, corresponding to surface silanol groups. Moreover, absorptions in the lower wavenumber region pertain to the generation of metal oxides, as Cu and Fe were integrated onto the silicon matrix; thus, the absorption between 580–680 cm^{-1} corresponds to Fe–O and Cu–O stretching vibrations. Finally, a broad band between 3400–3450 cm^{-1} and a weak peak at 1630 cm^{-1} relate to O–H stretching and bending vibrations of water and/or surface hydroxyl groups. Therefore, the FTIR suggests that a Cu–Fe/SiO_2 composite was formed and that silica and silica functional groups were absorbed and created (Ning et al. 2018, Ren et al. 2020). The textural property surface area was assessed via BET surface area on a Micromeritics ASAP 2020, where nitrogen adsorption–desorption isotherms after degassing the sample at 150°C under vacuum were used to calculate specific surface area via the Brunauer–Emmett–Teller method. Such information provides an initial overview of the solid properties of the catalyst, which enhance the effectiveness of the catalyst during reaction, particularly for the degradation of

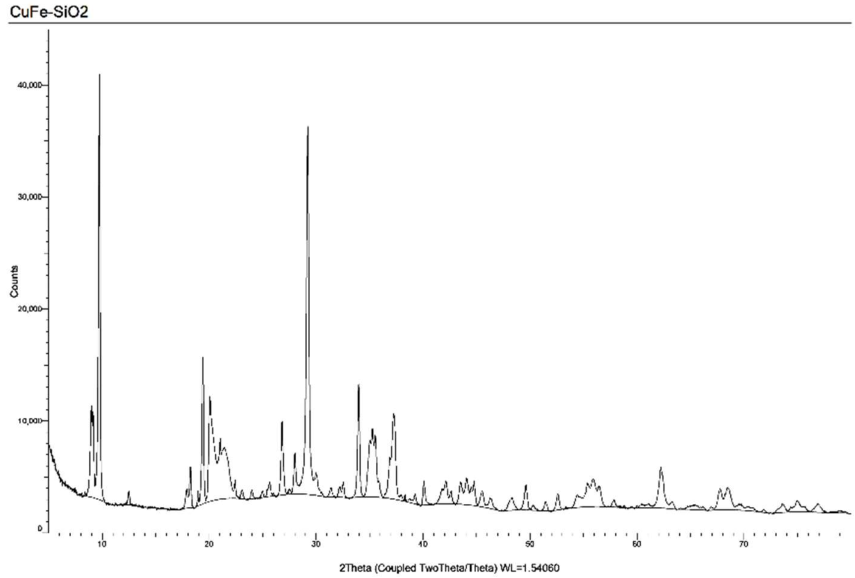

Fig. 1: XRD Spectrum of synthesized catalyst.

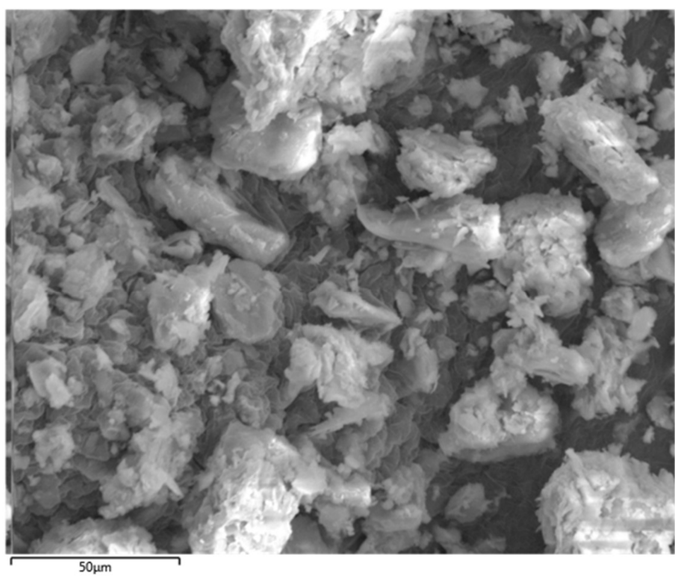

Fig. 2: SEM micrograph of the synthesized catalyst.

pharmaceutical wastewater. BET surface area measurement of the synthesized Cu–Fe/SiO_2 catalyst revealed a surface area of 111.1 $m^2.g^{-1}$. This indicates a porous structure of the catalyst, which is advantageous because this relatively large surface area possesses a high number of active sites. Better active dispersion of Cu and Fe during the heterogeneous Fenton-like oxidation reaction enhances the efficiency of pharmaceutical wastewater degradation (Guerreiro et al. 1997, Martínez et al. 2017, Sandhwar & Prasad 2017, Krupińska 2024, González-Castaño et al. 2021, Jia et al. 2022, Mekki et al. 2023, Salehzadeh et al. 2023).

2.5. Experimental Set-Up and Procedure

The current investigation was conducted within a 250 mL round-bottom three-necked glass reactor, wherein the central neck was sealed with a complete reflux system. During each trial, 100 mL of wastewater was introduced into the reactor along with the necessary amount of catalyst and H_2O_2, and then placed on a hot plate equipped with a magnetic stirrer. Various pH levels were tested; therefore, the initial pH of the mixture was adjusted using 1 M NaOH or 1 M H_2SO_4 prior to the addition of the catalyst and oxidant. Following

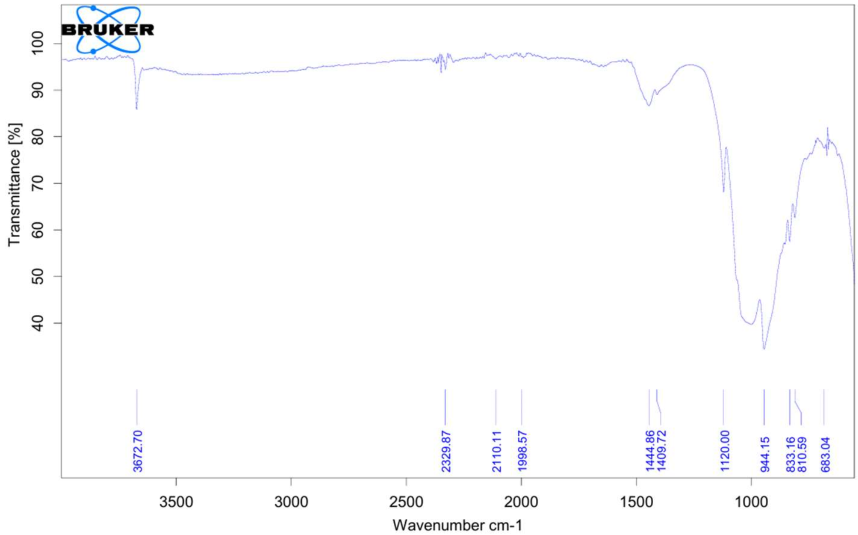

Fig. 3: FITR spectrum of the synthesized catalyst.

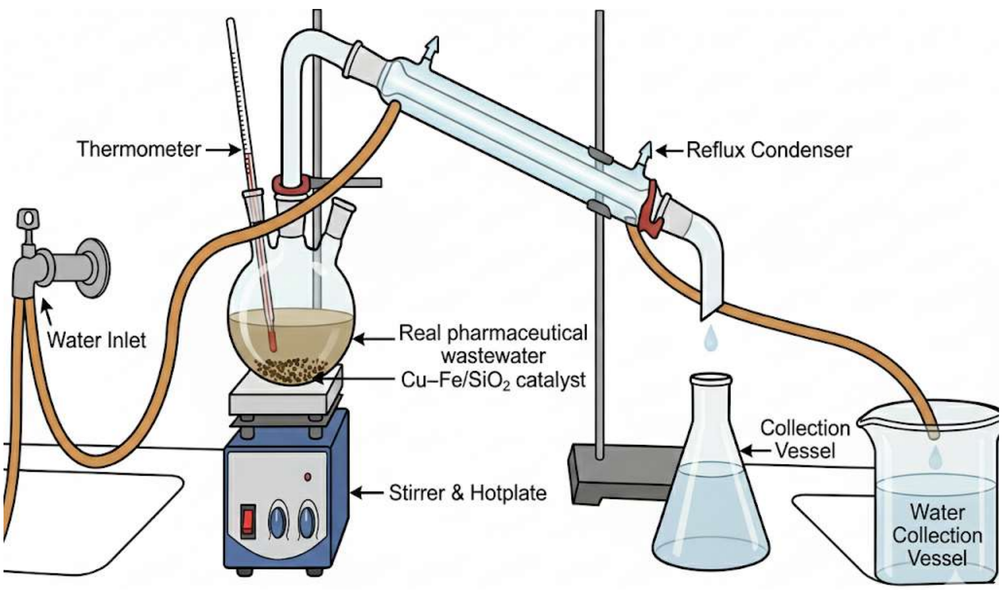

Fig. 4: Experimental setup.

the 3-h reaction period, 2 mL of supernatant was periodically extracted from the reactor and promptly filtered through a 0.22 μm Millex syringe filter. The resulting samples obtained were subsequently subjected to COD analysis using the APHA standard method. All procedures were repeated in duplicate, and the mean values were calculated with error bars indicating the standard deviation. Fig. 4 shows the experimental setup.

Preliminary trial experiments were carried out to determine appropriate operating ranges for key variables, namely catalyst dosage, H_2O_2 concentration, initial pH, and reaction time. These exploratory tests were essential to establish the upper and lower bounds for the subsequent optimization study. The finalized ranges of the independent variables are presented in Table 2. To systematically investigate the effects and interactions of these parameters on COD removal efficiency, Response Surface Methodology (RSM) was employed using a Central Composite Design (CCD). The experimental runs were arranged according to the CCD matrix, also summarized in Table 3, which incorporated various combinations of the independent variables (pH, catalyst dosage, and treatment time). This design framework enabled efficient modeling of the degradation efficiency and identification of optimal operating conditions.

3. RESULTS AND DISCUSSION

3.1. Effect of Catalyst Dosage, H_2O_2 Concentration, pH, and Reaction Time on COD Removal Efficiency

The effect of significant operating variables on COD removal efficiency via RSM is displayed in the three-dimensional surface plots seen in Fig.s 5 (a–f). For instance, catalyst dosage is shown to have a significantly positive contribution to COD removal, but to an extent, observing the contour plots, higher increases in catalyst loading from 0.4 $g.L^{-1}$ to 0.8 $g.L^{-1}$ increase degradation efficiency as more active Cu–Fe redox sites are available for subsequent H_2O_2 decomposition and •OH radical formation. However, anything beyond that can lead to radical scavenging means or serious aggregation of catalyst particles, which can reduce efficiency (Kumar et al. 2011, Yuan et al. 2022). Furthermore, the concentration of H_2O_2 has a significant concern of COD removal; raising increases in dosage from 30 to 80 $mg.L^{-1}$ increases efficiencies as it opens up more reagent for •OH formation. However, just like with the catalyst loading, excess loading of H_2O_2 can lead to a radical scavenging effect as HO_2• occurs. Since HO_2• has a lower oxidation potential, productivity also reduces. The pH has an adjusted impact on COD removal efficiency, as the lowest pH (pH 4–5) provides the highest efficiency. At low pH, iron and copper remain in a soluble form as redox-active, thus having a high activity in the Fenton-like reactions (Singh et al. 2013). However, neutral pH induces ferric hydroxide precipitation, which reduces active sites available and diminishes catalytic activations. The fact that both Fe^{3+}/Fe^{2+} and Cu^{2+}/Cu^{+} cycles operate well in the acidic pH domain (pH 3–4) means activated H_2O_2 and - OH maximization occurs. This is because at a low pH, Fe^{2+} stays soluble and can effectively engage H_2O_2, while the Cu sites regenerate $Fe^{3+} \rightarrow Fe^{2+}$ relatively easily. Thus, this sustains the dual redox cycle; however, as pH increases, Fe^{3+} precipitation occurs, and Cu speciation becomes more complex, meaning that electron transfer becomes more difficult and - OH is reduced. This explains why the COD removal is most effective in the mildly acidic window and less effective outside of it; discuss this mechanistic relationship (Fischbacher et al. 2017, Liu et al. 2018, Maekawa et al. 2014, Walling et al. 2021). Additionally, SiO_2 is a high-surface-area support that is chemically inert. This means that it stabilizes Cu and Fe oxide species and provides dispersed surface redox sites that are not aggregated. Silica coating or dispersion increases particle stability in aqueous environments, minimizes metal leaching, and SiO_2 can tune surface charge, which will both impact pollutant adsorption and the H_2O_2 approach to active sites. Thus, relate the activity and low leaching to improved dispersion and stabilization of Cu–Fe sites on SiO_2 but

Table 2: Variables and their levels obtained from the statistical software.

Central Composite Design characteristics				
Levels	Parameters (Range)			
	A	B	C	D
	Catalyst dosage [$g.L^{-1}$]	H_2O_2 concentration [mM]	Initial pH	Reaction time [min]
-2α	0.2	5	3	15
-α	0.4	30	4	45
0	0.6	55	5	75
+α	0.8	80	6	105
+2α	1	105	7	135

Table 3: CCD predicted set of experiments.

Run No.	A	B	C	D
1	0.4	30	4	45
2	0.8	30	4	45
3	0.4	80	4	45
4	0.8	80	4	45
5	0.4	30	6	45
6	0.8	30	6	45
7	0.4	80	6	45
8	0.8	80	6	45
9	0.4	30	4	105
10	0.8	30	4	105
11	0.4	80	4	105
12	0.8	80	4	105
13	0.4	30	6	105
14	0.8	30	6	105
15	0.4	80	6	105
16	0.8	80	6	105
17	0.2	55	5	75
18	1	55	5	75
19	0.6	5	5	75
20	0.6	105	5	75
21	0.6	55	3	75
22	0.6	55	7	75
23	0.6	55	5	15
24	0.6	55	5	135
25	0.6	55	5	75
26	0.6	55	5	75
27	0.6	55	5	75
28	0.6	55	5	75
29	0.6	55	5	75
30	0.6	55	5	75

do not relate it to any Fenton activity of the support itself (Martínez et al. 2017, Ning et al. 2018, Ren et al. 2020). Furthermore, the time factor has a slight impact on COD removal as efficiencies gradually change during 45–105 min. A longer reaction time allows for the effective blend between the catalyst and oxidant to ensure proper mineralization of the organics (Aghazadeh et al. 2023, Zhang et al. 2017, Ruziwa et al. 2023, Huilin et al. 2025). Yet, after 90 min, the reduction begins to plateau, which signifies saturation of active sites and reduced transferable biogenic organic matter. The reasons for the plateau in COD removal after ~90 min can be attributed to these aspects because (i) radical/oxidant depletion: bulk H_2O_2 concentration decreases and the effective steady-state •OH flux decreases; (ii) formation of recalcitrant intermediates: partially oxidized species that are less reactive with •OH can grow in concentration to prevent further mineralization; and (iii) mass-transfer limitations: general slower diffusion of remaining organics to active surface sites or blocked pores/sites from oxidation by-product adsorption. From an operational perspective, these can be countered by staged H_2O_2 dosing (maintaining available oxidants), improved hydrodynamics (external mass-transfer resistance minimized), periodic catalyst regeneration (surface fouling removed) (Kwan & Voelker 2002, Ban et al. 2020, Fischbacher et al. 2017, Krupińska 2024). Thus, all interactions better suggest that optimal COD removal (~76%) occurs at optimal catalyst loading (0.68 $g.L^{-1}$), H_2O_2 concentration ($\approx$65 $mg.L^{-1}$), weakly-acidic pH ($\approx$5.0), and reaction time of $\approx$86 min. This also suggests that properly balanced operations yield effective efficiencies without excessive reagents.

Table 4 illustrates that the comparative performances of Fenton and Fenton-like systems are closely influenced by the catalysts' composition, support materials, and operational conditions. Kaya and Asci (2022) reported an 86% COD removal from textile wastewater using an Fe/SnO_2 heterogeneous Fenton catalyst at pH 2 within 90 minutes, highlighting that iron-based systems can achieve exceptionally high efficiency under strongly acidic conditions. Zhao et al. (2017) evaluated the Fe_2O_3/SiO_2 catalyst for phenol degradation, resulting in a moderate COD removal of 64.6% at pH 3 over 60 minutes; the silica support stabilizes iron sites but offers relatively lower activity. Ban et al. (2020) employed a photo-Fenton system (Fe–Ce/Al_2O_3) on p-nitrophenol wastewater, attaining 72.9% COD removal at pH 4 after 120 minutes. Phong and Loc (2025) achieved increased efficiency with an rGO/nZVI heterogeneous Fenton catalyst, removing 81.5% COD from textile wastewater at pH 3 in 110 minutes, due to enhanced electron transfer and increased surface area. Su et al. (2018) reached an exceptional 99.8% COD removal using NZVI@ACF for cutting fluid wastewater at pH 5, though such nanostructured systems may involve higher costs and recovery challenges. Conversely, above 93% COD removals were attained within relatively short times by homogeneous Fe^{2+}/H_2O_2 systems reported by Ghjair and Abbar (2023) and Ayoub (2022). Overall, the comparison underlines the trade-off of efficiency versus operational sustainability, and it becomes increasingly relevant to apply heterogeneous supported Fenton catalysts for wastewater treatment.

3.2. Catalyst Reusability Study

To investigate the economic practicality of the heterogeneous Fenton-like process, the stability of CuFe/SiO_2 was assessed under optimized conditions (catalyst dosage 0.68 $g.L^{-1}$; pH 4.9; H_2O_2 concentration 65.28 mM; reaction time 86.81 min). During the first cycle, the catalyst operated with maximum functionality (74.11% COD removal) since all active surface

Table 4: Comparison of reported Fenton and heterogeneous Fenton-like catalysts for wastewater treatment.

Catalyst/system	Metal type	Support/configuration	Wastewater/ pollutant	pH	COD (or target) removal [%]	Time [min]	Ref.
Fe/SnO_2 heterogeneous Fenton	Fe	SnO_2	Textile wastewater	2	86	90	Kaya and Asci (2022)
Fe_2O_3/SiO_2 heterogeneous Fenton	Fe	SiO_2	Phenol solution	3	64.6	60	Zhao et al. (2017)
Fe–Ce/Al_2O_3 photoFenton	Fe–Ce	Al_2O_3	pNitrophenol wastewater	4	72.9	120	Ban et al. (2020)
rGO/nZVI heterogeneous Fenton	Fe^0	rGO (nanocomposite)	Textile wastewater	3	81.5 (Batch process)	110	Phong & Loc (2025)
NZVI@ACF/H_2O_2	Fe^0	Activated carbon fiber	Cuttingfluid waste	5	99.8	120	Su et al. (2018)
Homogeneous Fe^{2+}/H_2O_2	Fe^{2+}	– (homogeneous)	Hospital wastewater	3.1	95	93	Ghjair and Abbar (2023)
Homogeneous Fe^{2+}/H_2O_2	Fe^{2+}	– (homogeneous)	Industrial effluent (edible oil industry)	3	93.5	50	Ayoub (2022)

sites and Cu-Fe redox centers were open for reaction. The catalyst was separated via centrifugation after each run, washed with distilled water, dried, and reused without reactivation. It should be noted that the activity decreased slowly upon reusing it over four cycles, resulting in 69.78% in cycle 2, 60.21% in cycle 3, and 52.23% in cycle 4. The deactivated activity is in line with the expected trend for a heterogeneous Fenton catalyst. This includes partial leaching of active metal species during use as well as the gradual accumulation of recalcitrant carbonaceous residues on the catalyst, which limited the availability of active sites for reaction, as well as decreased effective hydroxyl radical formation. Such behavior has been widely documented for Cu-Fe-based mixed oxide systems under sequential oxidative use.

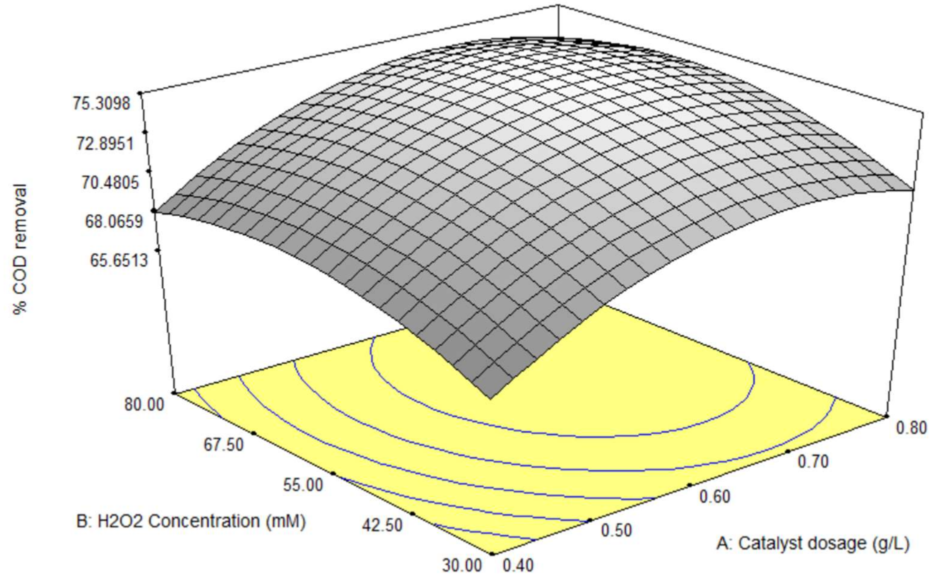

Fig. 5(a)

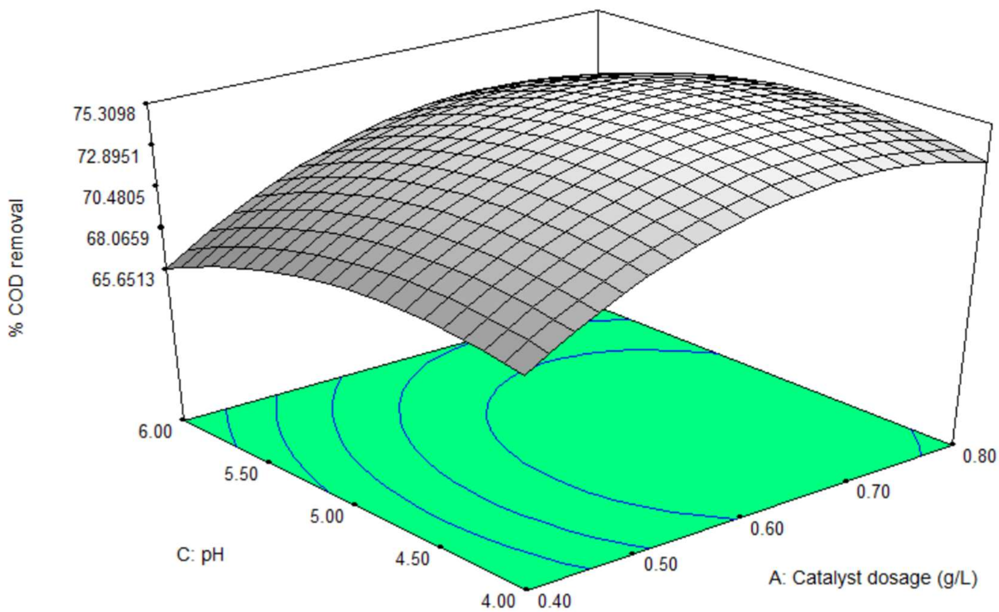

Fig. 5(b)

Figure Cont....

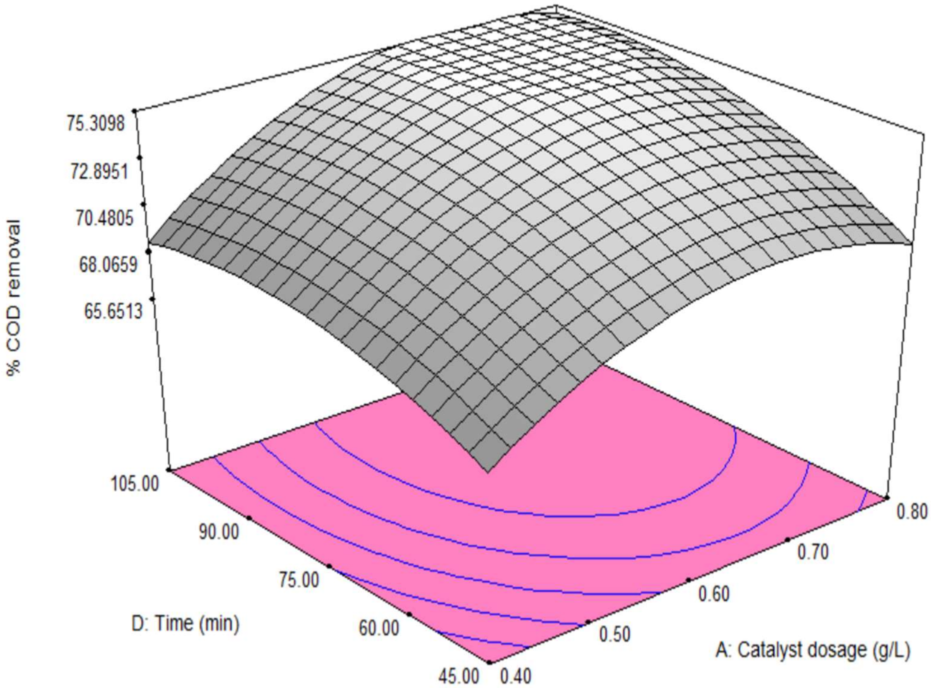

Fig. 5(c)

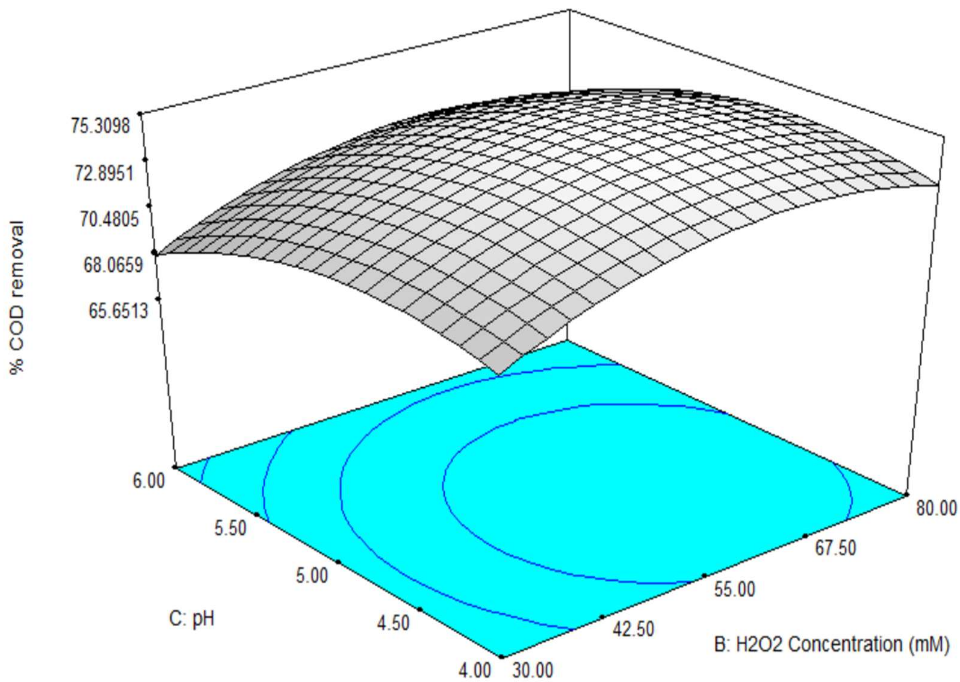

Fig. 5(d)

Figure Cont....

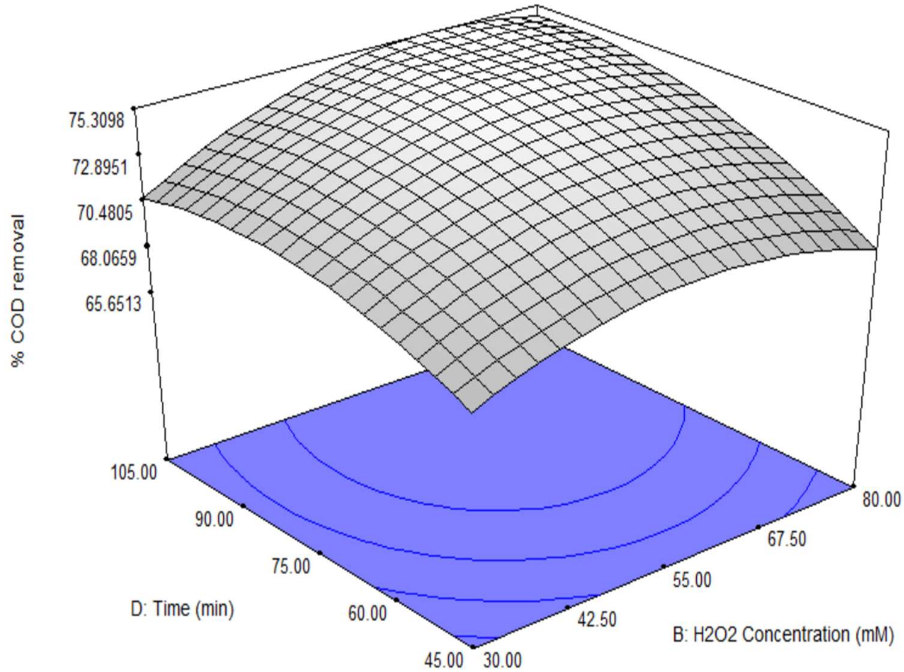

Fig. 5(e)

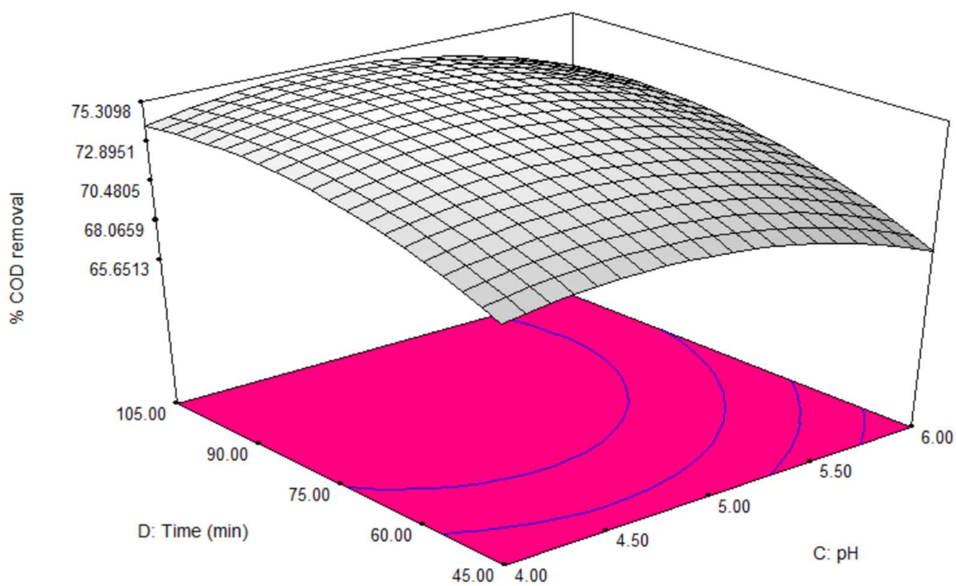

Fig. 5(f)

Fig 5: Effect of (a) catalyst dosage and H_2O_2 concentration, (b) catalyst dosage and pH, (c) catalyst dosage and time, (d) H_2O_2 concentration and pH, (e) H_2O_2 concentration and time, and (f) pH and time on % COD removal.

3.3. Radical Quenching, Reaction Mechanism, and Control Experiment Studies

To validate Cu-Fe/SiO_2 and heterogeneous Fenton-like mechanisms, radical quenching experiments were performed, which unambiguously identified hydroxyl radicals (- OH) as the main ROS contributing to pharmaceutical wastewater degradation at the optimal CCD experimental parameters. In radical quenching tests, tert-butanol (t-BuOH, 1- OH scavenger) and potassium iodide (KI, a scavenger for other non-radicals and bulk - OH) were added to solutions at 10 mM. In the Cu-Fe/SiO_2/H_2O_2 system, radical quenching was highly inhibited, with COD removal decreasing from 74.11% (based on the tested run) to 33.9%, equating to ~54% inhibition. Thus, it can be concluded that -OH radicals were the dominant oxidizing agents. On the other hand, quenching by KI resulted in a smaller inhibition of 11.6%, with efficiency reducing from 74.11% to about 62.51%. Thus, limited inhibition suggests that the Cu-Fe/SiO_2/H_2O_2 system occurs predominantly by •OH radicals confined to the surface at catalyst-active sites. Since KI acts predominantly on surface oxidative species and fails to effectively quench diffusing radicals (or homogeneous Fe-based) pathways, the absence of significant inhibition indicates that leached-Fe Fenton reactions, superoxide, or singlet oxygen do not significantly contribute as active species for the tested conditions (Li et al. 2015, Nath et al. 2022, Shao et al. 2022, Li et al. 2023).

The resulting mechanism occurs through three main steps.

(1) H_2O_2 activation via iron redox cycle (Wang et al. 2024, Hu et al. 2025):

Surface Fe^{3+} is first reduced by H_2O_2 to generate Fe^{2+}, and the formation of hydroperoxyl species (•OOH) follows Fenton activation as an occurrence of Fe^{2+} and H_2O_2 generating OH radicals (•OH) and regenerating Fe^{3+}, as shown in equations [1] and [2].

$$Fe^{3+} + H_2O_2 \rightarrow Fe^{2+} + \cdot OOH + H^+ \quad ...(1)$$

$$Fe^{2+} + H_2O_2 \rightarrow Fe^{3+} + \cdot OH + OH^- \quad ...(2)$$

(2) Synergistic Cu-Fe redox shuttle (Faheem et al. 2018, Wang et al., 2024, Hu et al. 2025):

Cu^{2+}/Cu^+ couples with Fe^{3+}/Fe^{2+} on the catalyst surface, making electron transfer easier and thus accelerating the Fe^{2+} regeneration step, where Cu^+ facilitates a faster approach and even activates H_2O_2 as well to create more •OH than inherently produced, as shown in equations [3] and [4].

$$Cu^{2+} + Fe^{2+} \leftrightarrow Cu^+ + Fe^{3+} \quad ...(3)$$

$$Cu^+ + H_2O_2 \rightarrow Cu^{2+} + \cdot OH + OH^- \quad ...(4)$$

(3) Pharmaceutical pollutant degradation (Thomas et al. 2021, Jiang et al. 2026):

The lattice-confined •OH produced at the Cu-Fe sites oxidizes the adsorbed pharmaceutical organics. Successive radical reactions create ring-opening, fragmentation and finally mineralization to CO_2 and other inorganic residues.

Control experiments confirmed the heterogeneous nature of the Cu-Fe/SiO_2/H_2O_2 system. When the reaction was conducted with H_2O_2 alone, only a minimal COD removal of approximately 7.6% was observed, indicating that H_2O_2 self-decomposition contributed little to oxidation. Similarly, using the catalyst without H_2O_2 resulted in a COD reduction of 5.8%, implying that adsorption or non-radical catalysis had a limited impact (Ksibi 2006, Erasmus et al. 2016, Aljuboury et al. 2017, Kwan & Voelker 2002). For example, to further assess the effect of soluble metal species, the reaction filtrate was tested under similar conditions after centrifugation to remove the catalyst; the resulting filtrate showed only 6.1% COD removal, indicating that leached Fe or Cu ions played a negligible role in oxidation (Ksibi 2006, Thomas et al. 2021, Jiang et al. 2026). Thus, collectively, these findings support the conclusion that the catalytic activity of Cu and Fe primarily arises from surface-confined Cu-Fe redox-active sites and that Cu-Fe/SiO_2/H_2O_2 operates via a genuine heterogeneous Fenton-like process rather than a homogeneous one (Li et al. 2015, Jiang et al. 2026).

3.4. Optimization Study and ANOVA Analysis

Table 5 presents both the CCD-predicted and experimental % COD removal results under optimal operating conditions. The RSM optimization of COD removal efficiency, along with the ANOVA statistics, validates the accuracy and predictability of the quadratic model. The model demonstrates a high coefficient of determination (R^2 = 0.9881), indicating it explains over 98% of the variance in COD removal. The adjusted R^2 (0.9769), closely aligned with R^2, suggests minimal loss of accuracy due to the number of predictors. Additionally, the predicted R^2 (0.9572) correlates strongly with the adjusted R^2, reflecting consistent reliability in predicted values. The low standard deviation (0.78) and coefficient of variation (C.V. = 1.15%) highlight excellent precision and repeatability of the experiments. The Adeq Precision value (31.677), which surpasses the threshold of 4, indicates an adequate signal-to-noise ratio. Finally, the low PRESS value (32.34) further confirms the model's strong predictability (Sarrai et al. 2016, Deepa et al. 2021, Pasciucco et al. 2025). The F-value of 88.74, with a p-value less than 0.0001, confirms that the quadratic model is highly significant. The final results of the quadratic equation [5], based on coded factors, indicate that catalyst dosage (A), H_2O_2 concentration (B), and reaction time (D) positively influence COD removal, while pH (C) has a marginally negative effect. Additionally, all squared terms (A^2, B^2, C^2, D^2) have negative coefficients, suggesting the presence of curvature and an optimal point rather than a purely linear relationship among all variables. Notably, the interaction terms AD and BD are significantly influential in determining COD removal efficiency, implying these variables work together to enhance removal capacity. The positive linear coefficients for A, B, and D suggest maximum COD removal occurs with increases in these factors, which then plateau. The negative quadratic terms for all four factors indicate that extreme values—such as excessive catalyst, oxidant, or reaction time—do not result in greater removal, likely due to radical saturation and scavenging effects. Among the interactions, the highest coefficient is for B and D (0.77 BD), highlighting that H_2O_2 dosage and reaction time are the most interactive parameters. Conversely, the relatively small coefficients for interactions AB, AC, and BC suggest these parameters are less interdependent, functioning more independently. Overall, this CCD effectively identifies optimal conditions for maximizing COD removal.

Ultimately, these optimization findings suggest that the resultant quadratic model is statistically valid, for it is clear that the optimized conditions yield maximum COD removal (~76%) with only moderately adjusted conditions. In conclusion, findings from these optimization steps indicate that the established quadratic model is statistically significant and optimized conditions result in maximum COD removal (~76%) with balanced operating conditions.

Final equation in terms of coded factors:

$$\%COD\ removal = 74.62 + 2.54\ A + 1.23\ B - 1.22\ C + 1.94\ D - 3.07\ A^2 - 2.15\ B^2 - 1.95\ C^2 - 1.70\ D^2 - 0.00125\ (A^*B) + 0.19\ (A^*C) + 0.57\ (A^*D) + 0.043\ (B^*C) + 0.77\ (B^*D) + 0.29\ (C^*D) \quad ...(5)$$

Where: A = Catalyst dosage ($g.L^{-1}$), B = H_2O_2 concentration (mM), C = pH, D = Reaction time (min)

4. CONCLUSIONS

This study demonstrates the effectiveness of a Cu–Fe/SiO_2 heterogeneous Fenton-like catalyst for the treatment of real pharmaceutical wastewater. Using CCD-based response surface methodology, it was found that COD removal is primarily influenced by catalyst dosage, H_2O_2 concentration, pH, and reaction time. Under optimized conditions, 0.68 $g.L^{-1}$ catalyst, 65.28 mM H_2O_2, pH 4.9, and 86.81 minutes, a COD removal of 76% was achieved. The correlation between experimental and predicted values was highly significant (P<0.0001), indicating that the quadratic model accurately describes the process (R^2 = 0.9881). Compared to traditional single-metal catalysts like Cu/Fe or unsupported variants reported in the literature, Cu–Fe/SiO_2 offers better active-site dispersion, reduced metal leaching, and enhanced •OH generation on the surface, making it more suitable for complex pharmaceutical effluents. Nonetheless, some limitations exist. Catalyst deactivation over multiple cycles suggests metal leaching or surface fouling, highlighting the need for regeneration and assessment of long-term stability under continuous operation. Future work should include cost analysis, lifecycle assessment of spent catalysts' environmental impact, and pilot-scale studies prior to practical application. Overall, these results confirm that Cu–Fe/SiO_2 is an effective and durable heterogeneous Fenton-like catalyst for sustainable pharmaceutical wastewater treatment, paving the way for its deployment in real-world scenarios.

5. ACKNOWLEDGMENTS

The authors gratefully acknowledge Parul University, Vadodara, for providing the necessary resources, research facilities, and support to carry out this work.

6. REFERENCES

Aghazadeh, M., Hassani, A.H. and Borghei, M., 2023. Application of photocatalytic proxone process for petrochemical wastewater treatment. *Scientific Reports*, 13(1), p.12738.

Ahidjo, N., Moanono, P., Boudem, C. and Kengne, F.L., 2024. Pharmaceutical residues in fish and macroinvertebrates around the wastewater treatment plant site at the University Teaching Hospital of Yaoundé, Cameroon. *Journal of Advances in Medical and Pharmaceutical Sciences*, 26(11), pp.66–77.

Alfarsi, A., Kumar, A., Gismelseed, A.M., Al Azkawi, A., Al Mahdouri, M., Al Mabsali, F.N. and Nugegoda, D., 2025. Pharmaceuticals and radiopharmaceuticals in wastewater treatment plants: insights from an Arabian Peninsula nation. *Environmental Science and Pollution Research*, pp.1–28.

Aljuboury, D.A.A., Palaniandy, P., Abdul Aziz, H.B. and Feroz, S., 2017. Degradation of total organic carbon (TOC) and chemical oxygen demand (COD) in petroleum wastewater by solar photo-Fenton process. *Global NEST Journal*, 19(3), pp.430–438.

Ayoub, M., 2022. Fenton process for the treatment of wastewater effluent from the edible oil industry. *Water Science & Technology*, 86(6), pp.1388–1401.

Ban, F.C., Zheng, X.T. and Zhang, H.Y., 2020. Photo-assisted heterogeneous Fenton-like process for treatment of PNP wastewater. *Journal of Water, Sanitation and Hygiene for Development*, 10(1), pp.136–145.

Bellouard, C., Kim, S., Ghanbaja, J., Wojcieszak, R., Canilho, N. and Pasc, A., 2024. Unraveling oxidation and spin states of a single Fe-based meso-macroporous silica catalyst in Fenton-like reaction by magnetic measurements. *The Journal of Physical Chemistry C*, 128(20), pp.8449–8457.

Table 5: CCD predicted optimum operating conditions and their experimental and CCD results.

Catalyst dosage [$g.L^{-1}$]	H_2O_2 concentration [mM]	pH	Time [min]	% COD removal	
				CCD (Pre.)	Test Run
0.68	65.28	4.9	86.81	76.07	74.11

Bravo-Suarez, J.J., Patil, B.S. and Pratt, S.R., 2025. In situ Raman spectroscopic study on the titania promotion of silica-supported tungsten catalysts for enhanced propylene metathesis. *Catalysis Today*, 447, p.115138.

Chen, W., Li, R.Y., Wang, C., Ji, M., Fu, L.W. and Satoshi, N., 2013. Advanced treatment of industrial wastewater by heterogeneous Fenton reaction using a novel composite catalyst. *Asian Journal of Chemistry*, 25(4), pp.3313–3317.

Chen, X., Yao, L., Xu, S., He, J., Li, N., Li, J., Liu, B., Zhu, Y., Chen, X., Wang, H. and Zhu, R., 2024. Electron transfer mediated photo-Fenton-like synergistic catalysis of Fe, Cu-doped MIL-101 coupled with Ag_3PO_4: quantitative evaluation and DFT calculations. *Environmental Pollution*, 351, p.124083.

Dai, W., Pang, J.W., Ding, J., Wang, Y.Q., Zhang, L.Y., Ren, N.Q. and Yang, S.S., 2023. Study on the removal characteristics and degradation pathways of highly toxic and refractory organic pollutants in real pharmaceutical factory wastewater treated by a pilot-scale integrated process. *Frontiers in Microbiology*, 14, p.1128233.

Deepa, R., Madhu, G., Thomas, R.M. and Achari, V.S., 2021. Removal of mefenamic acid from aqueous solution by Fenton process: optimization using response surface methodology with central composite design. *Nature Environment and Pollution Technology*, 20(5), pp.2061–2067.

Erasmus, E., Claassen, J.O. and Van Der Westhuizen, W.A., 2016. Catalytic wet peroxide oxidation of formic acid in wastewater with naturally-occurring iron ore. *Water SA*, 42(3), pp.442–448.

Faheem, M., Jiang, X., Wang, L. and Shen, J., 2018. Synthesis of Cu_2O–$CuFe_2O_4$ microparticles from Fenton sludge and its application in the Fenton process: the key role of Cu_2O in the catalytic degradation of phenol. *RSC Advances*, 8(11), pp.5740–5748.

Fischbacher, A., von Sonntag, C. and Schmidt, T.C., 2017. Hydroxyl radical yields in the Fenton process under various pH, ligand concentrations and hydrogen peroxide/Fe(II) ratios. *Chemosphere*, 182, pp.738–744.

Fu, Q., Malchi, T., Carter, L.J., Li, H., Gan, J. and Chefetz, B., 2019. Pharmaceutical and personal care products: from wastewater treatment into agro-food systems. *Environmental Science and Technology*, 53(24), pp.14083–14090.

Ghjair, A.Y. and Abbar, A.H., 2023. Optimization of Fenton process for removal of chemical oxygen demand (COD) from hospital wastewater using response surface methodology (RSM). *AIP Conference Proceedings*, 2787(1), p.040023.

González-Castaño, M., De Miguel, J.N., Sinha, F., Wabo, S.G., Klepel, O. and Arellano-Garcia, H., 2021. Cu supported Fe–SiO_2 nanocomposites for reverse water gas shift reaction. *Journal of CO_2 Utilization*, 46, p.101493.

Guerreiro, E.D., Gorriz, O.F., Rivarola, J.B. and Arrúa, L.A., 1997. Characterization of Cu/SiO_2 catalysts prepared by ion exchange for methanol dehydrogenation. *Applied Catalysis A: General*, 165(1–2), pp.259–271.

Hamieh, M., Tabaja, N., Chawraba, K., Hamie, Z., Hammoud, M., Tlais, S., Hamieh, T. and Toufaily, J., 2025. Visible light photo-Fenton with hybrid activated carbon and metal ferrites for efficient treatment of methyl orange (azo dye). *Molecules*, 30(8), p.1770.

Hu, Y., Zhou, Y., Ding, R., Ye, X., Chu, C., Liu, L.L., Tian, L., Jiang, X., Zhang, L.S., Zou, J.P. and Luo, S., 2025. Sustainable Fe and Cu sites double redox cycle boosting Fenton-like degradation of organic pollutants. *Environmental Science & Technology*, 59(31), pp.16812–16821.

Huilin, W., Saishengtai, G., Cheng, H. and Qin, Q., 2025. Enhancing Fenton oxidation for pharmaceutical wastewater. *International Journal of Agricultural and Environmental Information Systems*, 16(1), pp.1–15.

Jia, H., Lv, Q., Xia, Q., Hu, W. and Wang, Y., 2022. Tailoring the catalytic performance of Cu/SiO_2 for hydrogenolysis of biomass-derived 5-hydroxymethylfurfural to renewable fuels. *Frontiers in Chemistry*, 10, p.979353.

Jiang, S., Wu, C., Huang, Q., Yu, Y., Zhang, P., Wang, C., Ou, X. and Xu, M., 2026. Fe-Cu-loaded γ-Al_2O_3 as an efficient heterogeneous Fenton catalyst for the advanced treatment of petrochemical wastewater. *Water Cycle*, 7, pp.19–30.

Kaya, S. and Asci, Y., 2022. Heterogeneous Fenton process with Fe(III) based catalyst for treatment of textile industry wastewater. *Indian Journal of Chemical Technology*, 29(2), pp.166–173.

Khan, H.J., Ding, J., Qu, J., Sarrigani, G.V., Fitzgerald, P., Xu, X., Ghadi, A.E., Sui, Q., Tian, C., Cairney, J.M. and Wiley, D., 2025. Highly dispersed, single-atom cobalt, Fenton-like catalyst on microporous silica for efficient advanced oxidation process. *Applied Catalysis A: General*, 120469.

Kongkoed, P., Lertna, N., Athikaphan, P., Neramittagapong, A. and Neramittagapong, S., 2024. Enhancing catalyst stability: immobilization of Cu–Fe catalyst in sodium alginate matrix for methyl orange removal via Fenton-like reaction. *Heliyon*, 10(13), e33333.

Krupińska, I., 2024. Application of Fenton's reaction for removal of organic matter from groundwater. *Molecules*, 29(21), p.5150.

Ksibi, M., 2006. Chemical oxidation with hydrogen peroxide for domestic wastewater treatment. *Chemical Engineering Journal*, 119(2-3), pp.161–165.

Kumar, A., Prasad, B., Sandhwar, V.K. and Garg, K.K., 2021. Mechanistic insight into heterogeneous Fenton-like catalysis with M–Al_2O_3/SiO_2 (M = Fe, Co and Ni) for acrylonitrile mineralization from real ABS resin wastewater: optimization and toxicity assessment. *Journal of Environmental Chemical Engineering*, 9(3), p.105177.

Kumar, B.N., Anjaneyulu, Y. and Himabindu, V., 2011. Comparative studies of degradation of dye intermediate (H-acid) using TiO_2/UV/H_2O_2 and photo-Fenton process. *Journal of Chemical and Pharmaceutical Research*, 3(2), pp.718–731.

Kwan, W.P. and Voelker, B.M., 2002. Decomposition of hydrogen peroxide and organic compounds in the presence of dissolved iron and ferrihydrite. *Environmental Science & Technology*, 36(7), pp.1467–1476.

Li, J., Wei, Y., Liu, Q., Guan, H., Jiang, C. and Sun, X., 2025. Heterogeneous Fenton-like CuO-CoO_x/SBA-15 catalyst for organic pollutant degradation: synthesis, performance, and mechanism. *Frontiers in Chemistry*, 13, p.1552002.

Li, M., Song, J., Han, W., Yeung, K.L., Zhou, S. and Mo, C.H., 2023. Iron-organic frameworks as effective Fenton-like catalysts for peroxymonosulfate decomposition in advanced oxidation processes. *npj Clean Water*, 6(1), p.37.

Li, X., Liu, J., Rykov, A.I., Han, H., Jin, C., Liu, X. and Wang, J., 2015. Excellent photo-Fenton catalysts of Fe–Co Prussian blue analogues and their reaction mechanism study. *Applied Catalysis B: Environmental*, 179, pp.196–205.

Liu, X., Sang, Y., Yin, H., Lin, A., Guo, Z. and Liu, Z., 2018. Progress in the mechanism and kinetics of Fenton reaction. *MOJ Ecology and Environmental Sciences*, 3(1), pp.10–14.

Liu, X., Wang, L., Li, J., Li, R., He, R., Gao, W. and Yu, N., 2024. Preparation of heterogeneous Fenton catalysts Cu-doped MnO_2 for enhanced degradation of dyes in wastewater. *Nanomaterials*, 14(10), p.833.

Luo, Q., Wang, J., Wang, J., Shen, Y., Yan, P., Chen, Y. and Zhang, C., 2019. Fate and occurrence of pharmaceutically active organic compounds during typical pharmaceutical wastewater treatment. *Journal of Chemistry*, 2019(1), p.2674852.

Maekawa, J., Mae, K. and Nakagawa, H., 2014. Fenton- Cu^{2+} system for phenol mineralization. *Journal of Environmental Chemical Engineering*, 2(3), pp.1275–1280.

Martínez, F., Molina, R., Pariente, M.I., Siles, J.A. and Melero, J.A., 2017. Low-cost Fe/SiO_2 catalysts for continuous Fenton processes. *Catalysis Today*, 280, pp.176–183.

Mekki, S., Laichi, Y., Benourrad, F., Lagha, N., Chebout, R., Bachari, K. and

Saidi-Besbes, S., 2023. Copper triazole complex supported on Fe_3O_4@ SiO_2 nanoparticles as eco-friendly nanocatalysts in solvent-free Biginelli reaction. *Applied Organometallic Chemistry*, 37(8), e7103.

Munnik, P., De Jongh, P.E. and De Jong, K.P., 2015. Recent developments in the synthesis of supported catalysts. *Chemical Reviews*, 115(14), pp.6687–6718.

Nam, Y., Nam, D., Myung, Y., Joo, J.H. and Kim, C., 2025. Novel ferromagnetic $CuFe_2O_4$/Cu as a highly active catalyst for microwave-Fenton-like reaction. *npj Clean Water*, 8(1), p.56.

Nath, A., Biswas, S. and Pal, A., 2022. A comprehensive review on BPA degradation by heterogeneous Fenton-like processes. *Water Science & Technology*, 86(4), pp.714–745.

Nebot, C., Falcon, R., Boyd, K.G. and Gibb, S.W., 2015. Introduction of human pharmaceuticals from wastewater treatment plants into the aquatic environment: a rural perspective. *Environmental Science and Pollution Research*, 22(14), pp.10559–10568.

Ngoc, K.H.P. and Vu, A.T., 2022. Simple preparation of the CuO- Fe_3O_4/ silica composite from rice husk for enhancing Fenton-like catalytic degradation of tartrazine in a wide pH range. *Adsorption Science & Technology*, 2022, p.6454354.

Nguyen, T.B., Dong, C.D., Huang, C.P., Chen, C.W., Hsieh, S.L. and Hsieh, S., 2020. Fe-Cu bimetallic catalyst for the degradation of hazardous organic chemicals exemplified by methylene blue in Fenton-like reaction. *Journal of Environmental Chemical Engineering*, 8(5), p.104139.

Ning, J., Wang, M., Luo, X., Hu, Q., Hou, R., Chen, W., Chen, D., Wang, J. and Liu, J., 2018. SiO_2 stabilized magnetic nanoparticles as a highly effective catalyst for the degradation of basic fuchsin in industrial dye wastewaters. *Molecules*, 23(10), p.2573.

Omar, B.M., Zyadah, M.A., Ali, M.Y. and El-Sonbati, M.A., 2024. Pre-treatment of composite industrial wastewater by Fenton and electro-Fenton oxidation processes. *Scientific Reports*, 14(1), p.27906.

Pasciucco, E., Pasciucco, F., Panico, A., Iannelli, R. and Pecorini, I., 2025. Optimization of a Fenton-based process as a tertiary treatment of tannery wastewater through response surface methodology. *Journal of Water Process Engineering*, 69, p.106588.

Peralta-Ladino, Y.M., Molina, R. and Moreno, S., 2025. Novel synthesis of iron-based catalysts stabilized by oxygen defects on silica derived rice husk. *Surfaces and Interfaces*, 108035.

Phong, L.H. and Loc, N.X., 2025. Heterogeneous Fenton treatment of textile wastewater using rGO/nZVI: batch and flow column evaluation. *Water Science and Engineering*.

Pratiwi, J., Lin, J.Y., Mahasti, N.N., Shih, Y.J. and Huang, Y.H., 2021. Fluidized-bed synthesis of iron-copper bimetallic catalyst (FeIIICuI@ SiO_2) for mineralization of benzoic acid in blue light-assisted Fenton process. *Journal of the Taiwan Institute of Chemical Engineers*, 119, pp.60–69.

Ren, Y., Shi, M., Zhang, W., Dionysiou, D.D., Lu, J., Shan, C., Zhang, Y., Lv, L. and Pan, B., 2020. Enhancing the Fenton-like catalytic activity of nFe_2O_3 by MIL-53(Cu) support: a mechanistic investigation. *Environmental Science & Technology*, 54(8), pp.5258–5267.

Ruziwa, D.T., Oluwalana, A.E., Mupa, M., Meili, L., Selvasembian, R., Nindi, M.M. and Chaukura, N., 2023. Pharmaceuticals in wastewater and their photocatalytic degradation using nano-enabled photocatalysts. *Journal of Water Process Engineering*, 54, p.103880.

Salehzadeh, F., Esmkhani, M., Zallaghi, M., Javanshir, S. and Dekamin, M.G., 2023. $CuFe_2O_4$@SiO_2@L-arginine@Cu(I) as a new magnetically retrievable heterogeneous nanocatalyst with high efficiency for 1,4-disubstituted 1,2,3-triazoles synthesis. *Scientific Reports*, 13(1), p.8675.

Sandhwar, V.K. and Prasad, B., 2017. A comparative study of electrochemical treatment of para-toluic acid (p-TA) from aqueous solution: process optimization and sludge analysis. *Water Conservation Science and Engineering*, 1(4), pp.257–270.

Sandhwar, V.K. and Prasad, B., 2017. Comparative study of electrocoagulation and electrochemical Fenton treatment of aqueous solution of benzoic acid (BA): optimization of process and sludge analysis. *Korean Journal of Chemical Engineering*, 34(4), pp.1062–1072.

Sandhwar, V.K. and Prasad, B., 2018. Comparison of electrocoagulation, peroxi-electrocoagulation and peroxi-coagulation processes for treatment of simulated purified terephthalic acid wastewater: optimization, sludge and kinetic analysis. *Korean Journal of Chemical Engineering*, 35(4), pp.909–921.

Sarrai, A.E., Hanini, S., Merzouk, N.K., Tassalit, D., Szabó, T., Hernádi, K. and Nagy, L., 2016. Using central composite experimental design to optimize the degradation of tylosin from aqueous solution by photo-Fenton reaction. *Materials*, 9(6), p.428.

Shao, S., Cui, J., Wang, K., Yang, Z., Li, L., Zeng, S., Cui, J., Hu, C. and Zhao, Y., 2022. Efficient and durable single-atom Fe catalyst for Fenton-like reaction via mediated electron-transfer mechanism. *ACS ES&T Engineering*, 3(1), pp.36–44.

Singh, C., Chaudhary, R. and Gandhi, K., 2013. Preliminary study on optimization of pH, oxidant and catalyst dose for high COD content: solar parabolic trough collector. *Iranian Journal of Environmental Health Science & Engineering*, 10(1), p.13.

Su, C., Cao, G., Lou, S., Wang, R., Yuan, F., Yang, L. and Wang, Q., 2018. Treatment of cutting fluid waste using activated carbon fiber supported nanometer iron as a heterogeneous Fenton catalyst. *Scientific Reports*, 8(1), p.10650.

Tajoli, F., Dolcet, P., Claas, S., Maliakkal, C.B., Wang, D., Kübel, C., Casapu, M., Fröba, M., Grunwaldt, J.D. and Gross, S., 2025. Confining the synthesis of palladium nanoparticles in mesoporous silicas for CO oxidation: the role of the support. *ACS Applied Nano Materials*, 8(7), pp.3289–3303.

Thomas, A., Gayathri, V.M., Pillai, S.P., Sankeerthana, M. and Mani, S., 2021. Treatment of pharmaceutical wastewater. *International Journal of Engineering Research and Technology*, 10, pp.733–736.

Thomas, N., Dionysiou, D.D. and Pillai, S.C., 2021. Heterogeneous Fenton catalysts: a review of recent advances. *Journal of Hazardous Materials*, 404, p.124082.

Tricoli, A., Righettoni, M., Krumeich, F., Stark, W.J. and Pratsinis, S.E., 2010. Scalable flame synthesis of SiO_2 nanowires: dynamics of growth. *Nanotechnology*, 21(46), p.465604.

Vainoris, M., Nicolenco, A., Tsyntsaru, N., Podlaha-Murphy, E., Alcaide, F. and Cesiulis, H., 2022. Electrodeposited Fe on Cu foam as advanced Fenton reagent for catalytic mineralization of methyl orange. *Frontiers in Chemistry*, 10, p.977980.

Walling, S.A., Um, W., Corkhill, C.L. and Hyatt, N.C., 2021. Fenton and Fenton-like wet oxidation for degradation and destruction of organic radioactive wastes. *npj Materials Degradation*, 5(1), p.50.

Wang, C., Zhang, W., Wang, J., Xia, P., Duan, X., He, Q., Sirés, I. and Ye, Z., 2024. Accelerating Fe(III)/Fe(II) redox cycling in heterogeneous electro-Fenton process via S/Cu-mediated electron donor-shuttle regime. *Applied Catalysis B: Environmental*, 342, p.123457.

Wang, N., Yang, Y., Gong, C., Liu, X., Wang, K., He, W., Li, C., Li, Z. and Li, L., 2025. Study of Fe/Cu composite Fenton-like catalyst in the treatment of antibiotic wastewater: preparation, application, degradation pathways and working mechanism. *Journal of Environmental Chemical Engineering*, 13(2), p.115926.

Xu, W., Zou, R., Jin, B., Zhang, G., Su, Y. and Zhang, Y., 2022. The ins and outs of pharmaceutical wastewater treatment by microbial electrochemical technologies. *Sustainable Horizons*, 1, p.100003.

Yang, L. and Xue, F., 2024. Treatment of antibiotic-containing pharmaceutical wastewater by the novel VUV/UV/Fenton process at near-neutral pH. *International Journal of Environmental Science and Technology*, 21(4), pp.3889–3898.

Yuan, R., Xia, Y., Wu, X., He, C., Qin, Y., He, C. and He, X., 2022. Efficient advanced treatment of coking wastewater using O_3/H_2O_2/Fe-shavings process. *Journal of Environmental Chemical Engineering*, 10(2), p.107307.

Zhang, N., Zhang, G., Huang, T., Chong, S. and Liu, Y., 2017. Fe_3O_4 and $Fe_3O_4/Fe^{2+}/Fe^0$ catalyzed Fenton-like process for advanced treatment of pharmaceutical wastewater. *Desalination and Water Treatment*, 93, pp.100–108.

Zhao, J., Peng, R., Pan, Y. and Tao, Y., 2017. COD removal from phenol solution by heterogeneous Fenton reaction using Fe_2O_3/SiO_2 catalysts: effects of calcination temperature on the catalyst properties. *Indian Journal of Chemical Technology*, 24(4), pp.424–429.